Int. J. Heat Mass Transfer. Vol. 13, pp. 1571–1582. Pergamon Press 1970. Printed in Great Britain

HEAT TRANSFER TO A FLOWING NON-GRAY RADIATING GAS: AN EXPERIMENTAL AND THEORETICAL STUDY

I. S. HABIB* and R. GREIF†

Department of Mechanical Engineering, University of California, Berkeley, California U.S.A.

(*Received* 11 *July* 1969 *and in revised form* 20 *January* 1970)

Abstract—The problem considered is the determination of the heat transfer in fully developed turbulent flow of a non-gray radiating gas in a circular tube. Experimental and theoretical results have been obtained and are in good agreement. The effects of radiation on the temperature profile and the Nusselt number are reported.

NOMENCLATURE

A, total band absorptance;
A_0, band width parameter;
B, radiation intensity;
C_1, C_2, C_3, band absorptance properties;
c_p, specific heat at constant pressure;
D, tube diameter;
D_2, exponential integral function;
E_2, exponential integral function;
°F, degrees Fahrenheit;
h, heat-transfer coefficient; enthalpy;
I, electric current;
K, thermal conductivity;
K_ω, absorption coefficient;
°K, degrees Kelvin;
Nu, Nusselt number;
P, pressure;
P_{actual}, pressure;
P_e, equivalent broadening pressure;
Pr, Prandtl number;
q, total heat flux;
q_0, total heat flux at the wall;
q_r, radiative heat flux;
r_0, tube inside radius;
Re, Reynolds number;
t, pressure broadening parameter, also temperature;
T, temperature;
u, local velocity in flow direction, also non-dimensional optical depth given by $C_0^2 Pr$;
x, coordinate measured in the direction of flow;
y, radial distance measured from the wall;

Greek symbols

α, thermal diffusivity, $K/\rho c_p$;
β, heating parameter;
γ, angle;
ε, eddy diffusivity;
λ, wavelength;
μ, dynamic viscosity;
ν, kinematic viscosity, μ/ρ;
ρ, density;
τ, shear stress.

Subscripts

b, bulk value;
c, condition at band center;
0, evaluated at wall;

* Presently, Associate Professor of Mechanical Engineering, University of Michigan, Dearborn Campus, Dearborn, Michigan.

† Associate Professor of Mechanical Engineering.

x, condition at location x;
ω, indicated monochromatic values.

Superscript

$+$, dimensionless quantities.

INTRODUCTION

IN THIS study we consider fully developed turbulent flow of a non-gray radiating gas in a circular tube. Thus, the problem we are concerned with is one of energy transfer by conduction, turbulent convection and radiation in a cylindrical medium. Because of the complexity of this problem, (see e.g. [1]) an analysis was previously carried out for the same system but under optically thin conditions [2]. Detailed calculations were made which demonstrated that a constant heat flux, constant shear stress formulation yielded results which were in very good agreement with results that were obtained from the basic equation for the conservation of energy. In a separate study it was also shown that nongray effects could be included in a radiating cylindrical medium through use of the total band absorptance [3]. On the basis of these studies more general theoretical results were obtained and are presented in this paper for the turbulent flow of a nongray radiating gas in a tube. A comparison was then made with experimental data obtained from tests conducted with carbon dioxide. As a check on our system, experiments were also carried out with air, a non-radiative participating gas at the temperatures of interest, and a comparison of experimental and theoretical results was made.

EXPERIMENTAL SYSTEM

The experimental system used in this study is shown schematically in Fig. 1 and a detailed drawing of the stainless steel test section is shown in Fig. 2. The tube is 22 ft long with an o.d. of 2·0 in. and a wall thickness of 0·049 in. The tube was heated by employing it as the resistance element of an electric circuit with electrodes attached at each end of the tube for

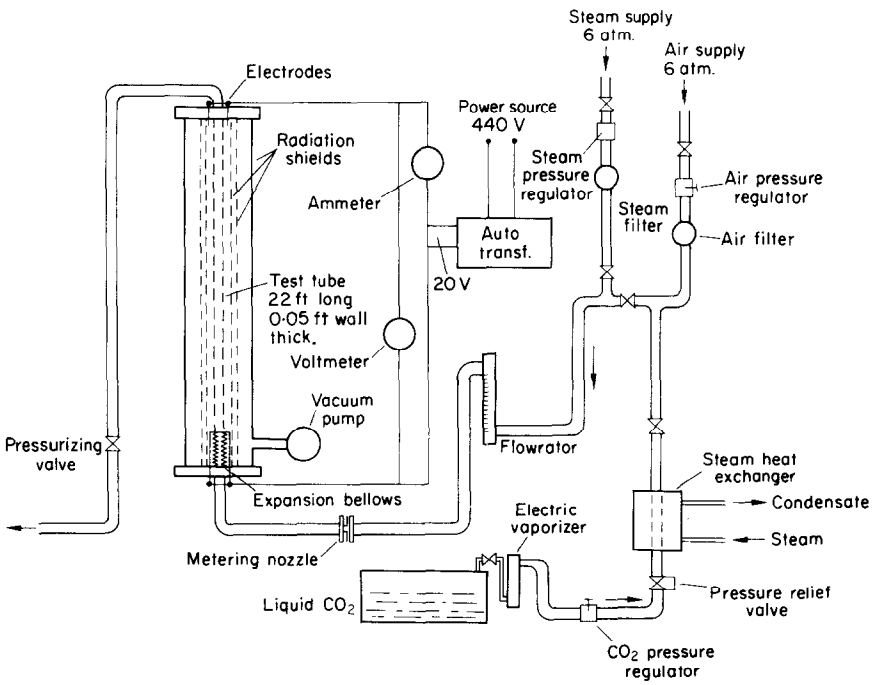

FIG. 1. Sketch of apparatus.

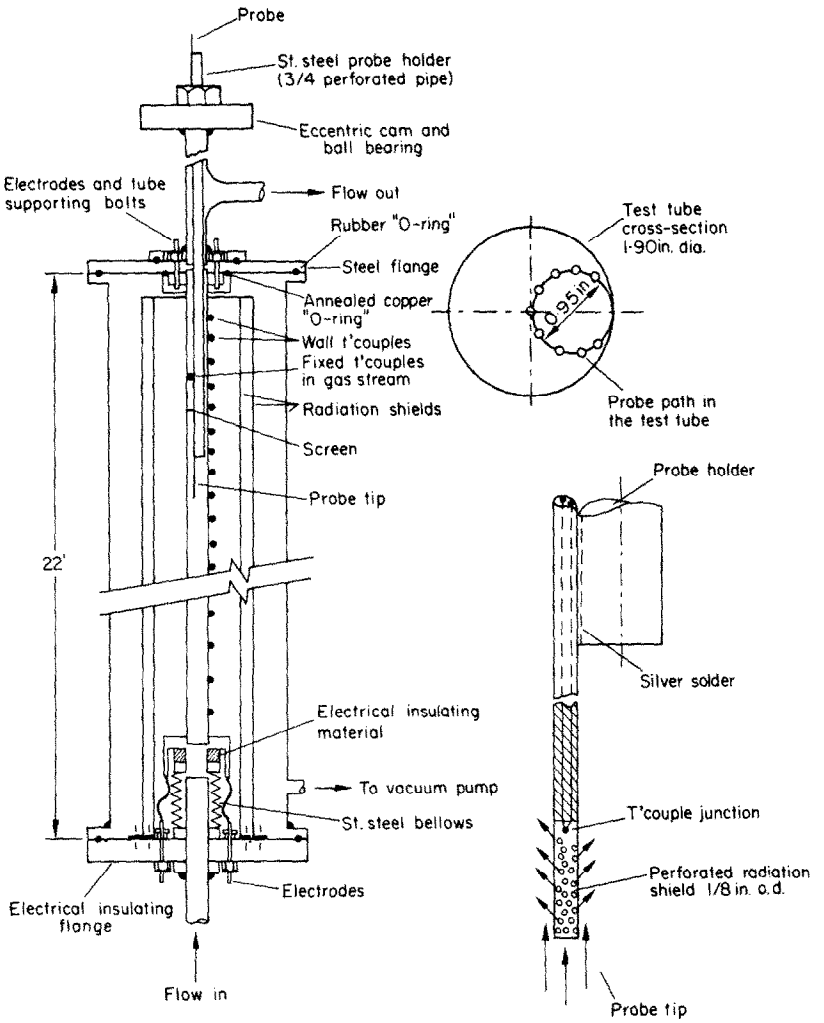

FIG. 2. Test tube.

this purpose. An a.c. power supply was used which was capable of stepping down the line voltage to 20 V with a current carrying capacity of 2500 A. However, because of the relatively fixed electrical resistance of the tube and the fixed output voltage of the power supply, a maximum electric current of approximately 425 A was obtained. The maximum wall temperature obtained was 750°F. With electric heating, the energy per unit area transferred from the tube to the gas was practically constant over the test section. The variation of the electrical resistivity of the tube with temperature resulted in a slight variation in the value of the energy generated. Furthermore, the radiation heat losses varied along the tube. The surface temperature of the tube increased gradually with axial distance in the direction of the flow (cf. Fig. 3).

To minimize natural convection losses the region surrounding the test tube was maintained in a vacuum of approximately 0·5 mm of

mercury. In addition, three steel tubes of diameters 10, 12 and 16 in. enclosed the test tube and acted as radiation shields. The primary heat losses in the system were due to radiation

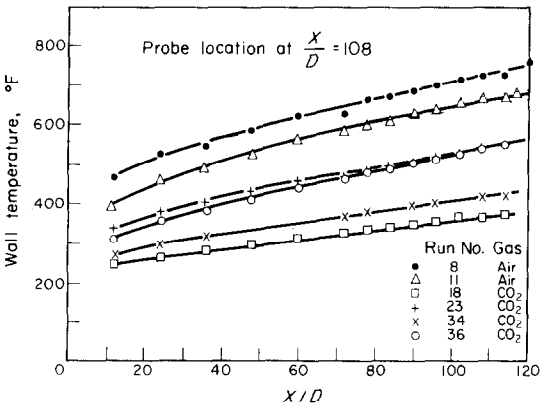

FIG. 3. Variation of wall temperature with axial distance.

transfer through the shields and conduction losses through the end flange. The entire apparatus stood vertically on a structural support and the tube was anchored to the outermost shield at the top by means of a steel flange. This allowed the tube to expand vertically downward upon heating. Another flange made up of electrically insulating hard fibers was used to connect the shields and the test tube at the bottom of the apparatus. To provide for the expansion of the tube, a stainless steel bellows was installed in the flow path and connected the tube inlet and the insulating flange. A steel pipe was inserted in the bellows to minimize any whirling motion of the gas as it entered the tube. The bellows was electrically insulated from the test tube. At the cool end of the system (lower end), rubber O-rings were used around the flanges and other connecting parts to obtain a satisfactory seal; at the hot end, an annealed copper ring was used.

The gas flowed through the test tube and was heated by the hot tube walls. In the case of air, the source of supply was a large air tank pressurized to approximately 6 atmospheres. The air was filtered to remove suspended oil and water droplets and then passed through a pressure regulator set at 50 psi. Flow control valves were mounted on the instrument panel to permit either air, carbon dioxide or steam to be used. These values also regulate the gas flow rate through the system. One control valve was used at the test tube discharge line in order to allow the gas in the tube to be pressurized. In the case of carbon dioxide, liquid CO_2 from a 750 lb tank maintained at 300 psi was passed through a vaporizer and then through a pressure regulator set at approximately 60 psi. The vaporized gas then passed through a steam heat exchanger to maintain a certain gas temperature at the test tube inlet.

All temperature measurements were made with chromel–alumel thermocouples and a "L&N" self-compensating temperature readout unit designed to read in degrees F. Thirty thermocouples were spot welded to the outer surface of the tube. The axial spacing of the thermocouples varied from 2 ft at the lower third of the tube to 6 in. at the upper third. On some axial locations, two thermocouples were situated opposite and at 90 degrees to each other to check any peripheral variation in the tube wall temperature. It was observed that no appreciable difference in measured wall temperature existed except near the tube outlet where axial conduction losses existed and these losses were apparently non-uniform. The thermocouple leads approached the measuring junction in opposite directions and parallel to the axis of the tube.

The centerline gas inlet temperature was measured with a thermocouple. In addition, a temperature probe was placed at an axial location of $x/D = 108$ to measure the hot gas temperature. This location is approximately $2\frac{1}{2}$ ft from the top of the tube. A stainless steel radiation shield* was placed around the probe. The o.d. of the shield was 0·125 in. and the shield

* An estimate of the error due to radiation was made and the result was a maximum temperature deviation of less than 2°F.

and the thermocouple were silver soldered together. Fine holes were drilled in the shield (cf. Fig. 2).

The probe thermocouple was made of chromel–alumel wire, 0·020 in. dia. and was insulated from the thermocouple sheath with ceramic ("Ceramo"). The entire probe is welded to a long $\frac{3}{4}$ in. dia. stainless steel pipe which is bolted to an eccentric cam attached to a ball bearing situated at the top of the tube. When the bearing rotates, the probe scans a path from the center of the tube toward the wall. A gear drive is incorporated so that the probe can be rotated from a location close to the instrument panel. The probe position was determined by using a counter that was calibrated against the various radial positions of the probe in the pipe.

The mass flow rate was measured using two ASME nozzles with 0·5 and 0·75 in. throat dia. and a flowrator. The metering nozzle is located approximately 5 ft ahead of the test tube entrance. A "Ü" tube water manometer was used for the measurement of the static pressure difference across the nozzle. During the low pressure runs, a "Ü" tube mercury manometer was used to measure the nozzle inlet pressure; for the high pressure runs a pressure gauge was used. Additional gauges were available to measure the tube inlet and outlet pressures. The electric current and the voltage drop were measured by an ammeter and a voltmeter, respectively.

NON-GRAY RADIATION TRANSPORT

In a previous study it was shown [3] that it was possible to include non-gray effects in a cylindrical medium. (For the planar medium refer to [4]–[6].) This was accomplished by incorporating the total band absorptance into the basic radiative transport equations. Exact results were obtained for this problem. These radiative transport calculations are quite complex. Furthermore, the problem is made increasingly difficult when we also consider a coupled radiating flow problem with variable properties. Because of these considerations, an approximate formulation for the radiation transport was also carried out using the approximation [3]

$$D_2(x) \equiv \int_0^{\pi/2} (\cos\alpha) \exp\left(\frac{-x}{\cos\alpha}\right) d\alpha = \int_0^1 \frac{\mu\, e^{-x/\mu}}{(1-\mu^2)^{\frac{1}{2}}} d\mu \approx a\, e^{-bx}$$

where a and b are arbitrary constants. Calculations were made using this approximation and a comparison between the approximate and the exact results was made. Excellent agreement was obtained for $a = 1$ and $b = \frac{5}{4}$.* Based on these results we therefore write the following approximate expression for the radiative flux:†

$$\begin{aligned} q_r = \frac{4a}{b} \int_{\gamma=0}^{\pi/2} \cos\gamma \Bigg\{ & \int_{r\sin\gamma}^{r} A\left[\frac{b(r-r')}{\cos\gamma}\right] \frac{d}{dr'} \\ & \times [B_{\omega c}(r') - B_{\omega c,0}]\, dr' + \int_{r}^{R} A\left[\frac{b(r'-r)}{\cos\gamma}\right] \frac{d}{dr'} \\ & \times [B_{\omega c}(r') - B_{\omega c,0}]\, dr' \\ & - \int_{r\sin\gamma}^{R} A\left[\frac{b(r+r'-2r\sin\gamma)}{\cos\gamma}\right] \frac{d}{dr'} \\ & \times [B_{\omega c}(r') - B_{\omega c,0}]\, dr' \\ & - [B_{\omega c}(R) - B_{\omega c,0}] \left(A\left[\frac{b(R-r)}{\cos\gamma}\right] \right. \\ & \left. - A\left[\frac{b(r+R-2r\sin\gamma)}{\cos\gamma}\right]\right) \Bigg\} d\gamma. \end{aligned} \tag{1}$$

* For the *planar* geometry, the approximation $E_2(x) \equiv \int_0^1 e^{-x/\mu} d\mu \simeq ce^{-dx}$ may be made and very good results are obtained for this case with $c = 0{\cdot}9$ and $d = 1{\cdot}8$ [6].

† We have taken the absorption coefficient, k_ω, to be independent of the temperature. However, for the case when k_ω is a function of the temperature according to $k_\omega = \text{fcn}(\omega) \cdot \text{fcn}(T)$ the same procedures can be carried out [5].

The total band absorptance, A, [7–9] is defined by

$$A(y) = \int_{\Delta\omega} [1 - e^{-k_\omega y}]\, d\omega \tag{2}$$

where $\Delta\omega$ is the band width. Note that q_r is the total radiative flux for one band which was obtained by integrating the spectral radiative flux over the band width:

$$q_r = \int_{\Delta\omega} q_{r\omega}\, d\omega.$$

In deriving equation (1) we considered the tube wall to be black and diffuse. Monochromatic measurements of the tube wall emissivity were made at room temperature and at a temperature of 900°F [10]. Calculations were then made for both the temperature profiles and the radiative flux profiles and the effect of emissivity was shown to be small [10]. In addition, the axial radiative flux is neglected. Note that our temperature profiles in the gas stream were measured at a location 108 diameters downstream (cf. Fig. 3).

In the analysis of turbulent flows the nondimensional distance $y^+ = (y/v_0)\sqrt{(\tau_0/\rho_0)}$ is used where $y = r_0 - r$. In terms of y^+ the radial radiative heat flux is then given by

$$q_{r,y^+} = \frac{4a}{b} \int_0^{\pi/2} \cos\gamma \left\{ \int_0^{r_0^+ + (r_0^+ - y^+)\sin\gamma} A\left[\frac{bC_0^2 Pr_0}{\cos\gamma r_0^+} \times (2r_0^+ - y^+ - y^{+\prime} - 2(r_0^+ - y^+)\sin\gamma)\right] \times \frac{d[B_{\omega c} - B_{\omega c,0}]}{dy^{+\prime}}\, dy^{+\prime} - \int_{y^+}^{r_0^+ - (r_0^+ - y^+)\sin\gamma} \times A\left[\frac{bC_0^2 Pr_0}{\cos\gamma r_0^+}(y^{+\prime} - y^+)\right] \frac{d[B_{\omega c} - B_{\omega c,0}]}{dy^{+\prime}}\, dy^+ - \int_0^{y^+} A\left[\frac{bC_0^2 Pr_0}{\cos\gamma r_0^+}(y^+ - y^{+\prime})\right] \times \frac{d[B_{\omega c} - B_{\omega c,0}]}{dy^{+\prime}}\, dy^{+\prime} \right\} d\gamma \tag{3}$$

Note that for problems that involve energy transport by both conduction and radiation, the last term in equation (1) is identically zero because of the continuity of temperature at the boundary. In general, the total radiative heat flux may be represented by

$$q_r = \sum_{i=1}^{N} q_{r,i}$$

where $q_{r,i}$ is the radiative heat flux for one vibrational–rotational band, given by equation (3), and N is the number of bands in the gas.

To evaluate the total band absorptance we use the following correlation of Tien and Lowder [8] based on the results of Edwards and Menard [7]:

$$A_i = A_{0,i} \ln\left\{\frac{u_i f(t_i)(u+2)}{[u_i + 2f(t_i)]} + 1\right\} \tag{4}$$

where

$$f(t_i) = 2{\cdot}94\,[1 - e^{-2{\cdot}6t_i}]. \tag{5}$$

Equation (4) is a curve fit to a three-region band absorptance formulation which is based upon an exponential wide band model for the absorption coefficient.

For carbon dioxide we consider the two strongest bands and list the pertinent radiation parameters in Table 1. The optical depth variable u_i is defined by

$$u_i = C_{0,i}^2 Pr \tag{6}$$

where $C_{0,i}^2$ is given by

$$C_{0,i}^2 = C_{1,i}/C_{3,i} RT. \tag{7}$$

In equation (5) t_i is a line structure parameter defined by

$$t_i = B_i^2 P_{e,i} \tag{8}$$

with

$$B_i^2 = C_{2,i}^2/4C_1C_3, \quad P_{e,i} = 2\,P_{\text{actual}}. \tag{9}$$

The above relation between the pressures is only valid when there is no foreign gas broadening.

Table 1. Radiative parameters for carbon dioxide (Tien [9])

Band center (cm^{-1})	C_1 (cm^{-1}/gm M^{-2})	C_2 (cm^{-1}/[gm M^{-2}]$^{\frac{1}{2}}$)	C_3 (or A_0) (cm^{-1})	Integrated intensity of band $(cm^2\text{-atm})^{-1}$
667	19	$6{\cdot}9(T/T_r)^{0{\cdot}5}$	$12{\cdot}9(T/T_r)^{0{\cdot}5}$	2970
2350	110	$31(T/T_r)^{0{\cdot}5}$	$11{\cdot}5(T/T_r)^{0{\cdot}5}$	240 ± 36

T_r = reference temperature = 100°K.

FULLY DEVELOPED TURBULENT FLOW OF A NON-GRAY RADIATING GAS

We are interested in determining the heat transfer to a radiating gas in turbulent flow. First, the velocity profile must be obtained from the momentum equation which, for variable properties, is coupled to the energy equation through the temperature dependence of the viscosity and the density. Deissler [11, 12] solved the coupled energy and momentum equations for fully developed turbulent flow. He concluded, from experimental and theoretical results, that the effect of variable shear stress and heat transfer on both the velocity and temperature distributions for a radiative non-participating gas was slight. In addition, Nichols [13] showed that the velocity profiles obtained in an annulus with steam, a radiating gas, agreed with those presented by Deissler. Nichols [13] also concluded that for heat-transfer calculations, equating the eddy diffusivities for momentum and for heat transfer is a good assumption. Therefore, for our problem we shall also use the velocity profiles and eddy diffusivities presented by Deissler [11, 12] (also, refer to Martinelli [14]).

In a previous study, the heat transfer in fully developed turbulent flow of an *optically thin* radiating gas was determined by solving the basic equation for the conservation of energy [2]. In addition, the constant (total) heat flux, constant shear formulation was also used and the resulting heat flux and temperature profiles were shown to be in very good agreement with those obtained from the energy equation [2]. On the basis of these results, the constant flux, constant shear formulation has been used in the present problem for a non-optically thin, frequency dependent radiating gas with variable properties.*

The total heat flux, q, is given by

$$q = -(K + \rho c_p \varepsilon)\frac{dT}{dy} + q_r \qquad (10)$$

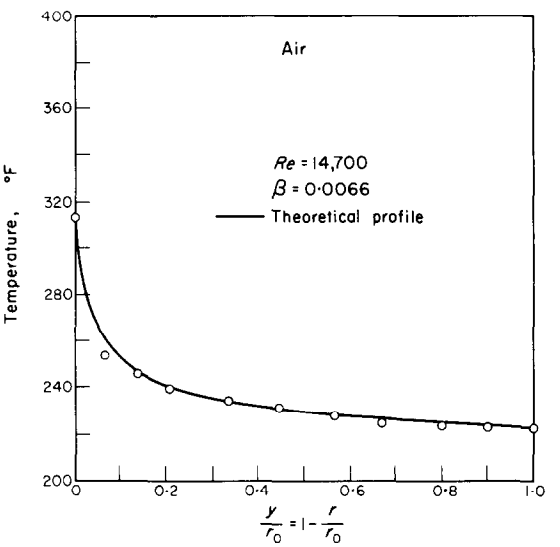

FIG. 4. Experimental and theoretical temperature profiles for air.

* It should be emphasized that to obtain the correct radiation transfer contribution in optically thin problems it is necessary to include both the Planck mean and the modified Planck mean coefficients [4, 15]. This requires the radiative properties to vary with temperature. In reference [2] this variation was allowed but all other properties, i.e. "conduction and convection properties" were taken to be independent of the temperature.

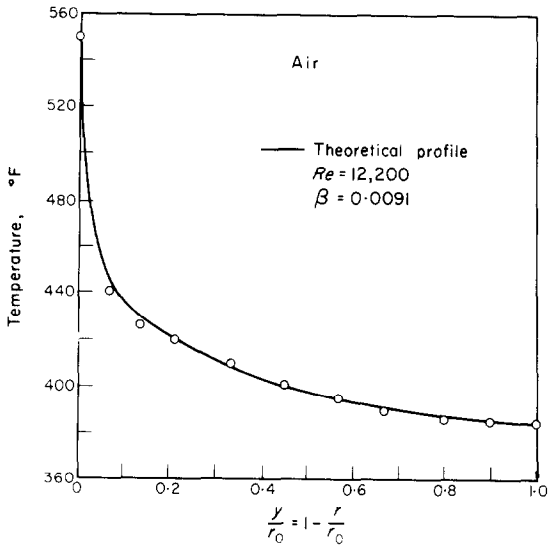

FIG. 5. Experimental and theoretical temperature profiles for air.

where q_r is the radiative flux defined in equation (3), ε is the eddy diffusivity and K is the thermal conductivity. We invoke the constant heat flux condition, $q/q_0 = 1$, and obtain

$$1 = \left(\frac{K/K_0}{Pr_0} + \frac{\rho}{\rho_0}\frac{\varepsilon}{\nu_0}\right)\frac{dT^+}{dy^+} + \frac{q_r}{q_0} \quad (11)$$

where the non-dimensional distance and temperature are given by

$$y^+ = \frac{y\sqrt{(\tau_0/\rho_0)}}{\nu_0}, \quad T^+ = \frac{1}{\beta}\left(1 - \frac{T}{T_0}\right) \quad (12)$$

with

$$\beta = \frac{q_0\sqrt{(\tau_0/\rho_0)}}{c_{p_0}\tau_0 T_0}. \quad (13)$$

The temperature dependence of the thermal conductivity and the viscosity is given by

$$\frac{K}{K_0} = \frac{\mu}{\mu_0} = \left(\frac{T}{T_0}\right)^m = (1 - \beta T^+)^m \quad (14)$$

with $m = 0{\cdot}69$ [16, 17].

The total turbulent shear stress is given by

$$\tau = (\mu + \rho\varepsilon)\frac{du}{dy}. \quad (15)$$

For constant shear stress this becomes

$$1 = \left(\frac{\mu}{\mu_0} + \frac{h}{\rho_0}\frac{\varepsilon}{\nu}\right)\frac{du^+}{dy^+} \quad (16)$$

where the dimensionless velocity is defined by

$$u^+ = u/\sqrt{(\tau_0/\rho_0)}. \quad (17)$$

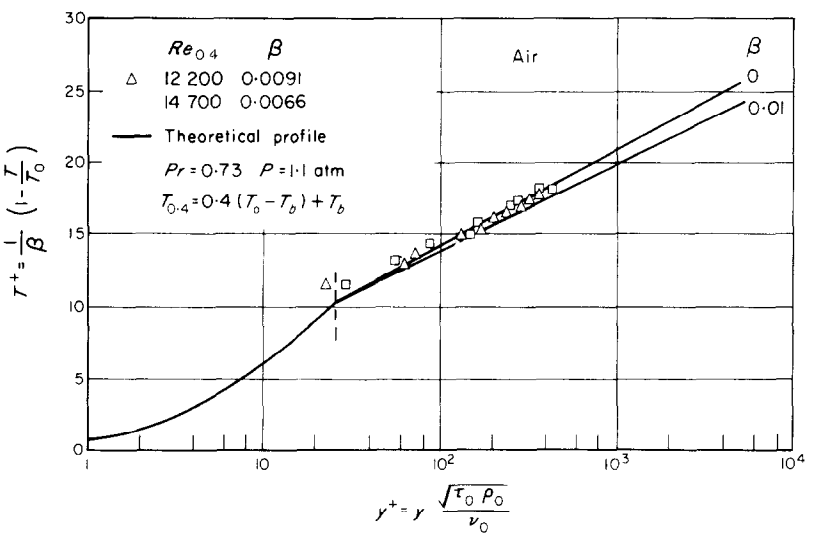

FIG. 6. Dimensionless temperature profiles for air.

Combining equations (11) and (16) we obtain

$$1 = \left[\frac{K}{K_0}\left(\frac{1}{Pr_0} - 1\right) + \frac{1}{du^+/dy^+}\right]\frac{dT^+}{dy^+} + \frac{q_r}{q_0}. \quad (18)$$

For convenience the velocity profiles of Deissler [11] were previously fitted using the following relations [18]:

$$\begin{aligned} u^+ &= y^+ && 0 < y^+ < 5 \\ u^+ &= a_1(\beta) + b_1(\beta)\ln y^+ && 5 < y^+ < 26 \quad (19) \\ u^+ &= a_2(\beta) + b_2(\beta)\ln y^+ && 26 < y^+ < r_0^+. \end{aligned}$$

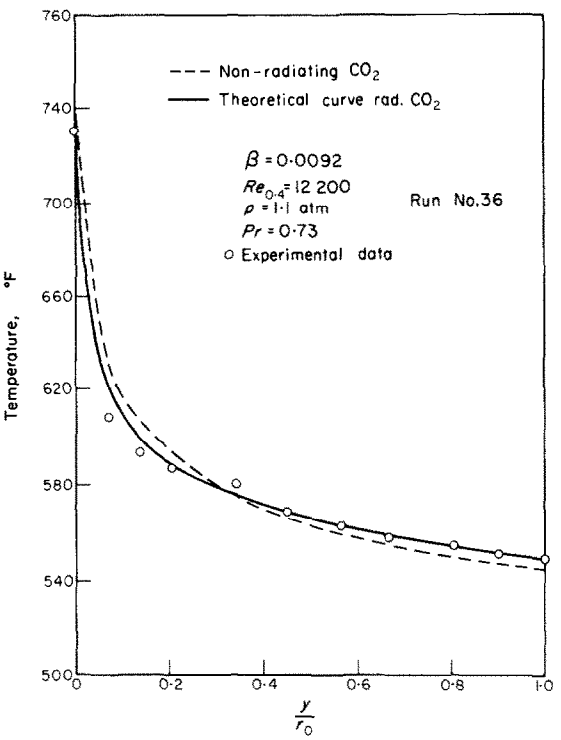

FIG. 7. Experimental and theoretical temperature profiles for carbon dioxide.

The functions of β in equation (19) are presented in [18]. Equation (18), in conjunction with the velocity profiles of equation (19), represents a completely specified problem. Equation (18)

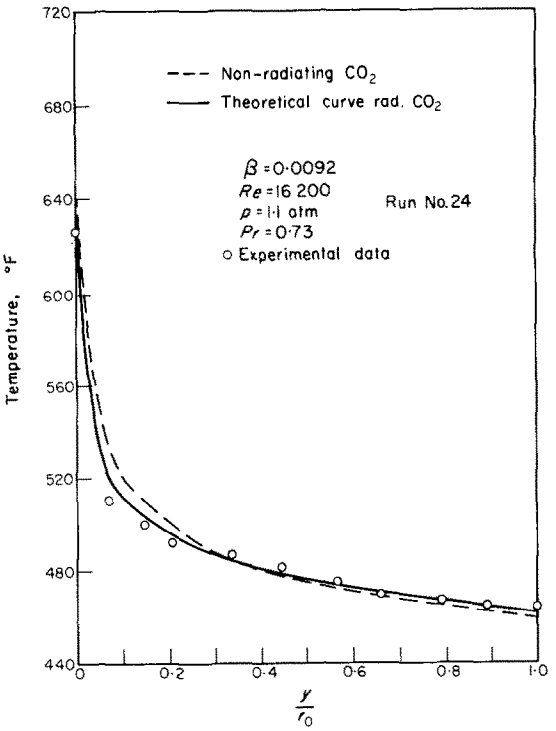

FIG. 8. Experimental and theoretical temperature profiles for carbon dioxide.

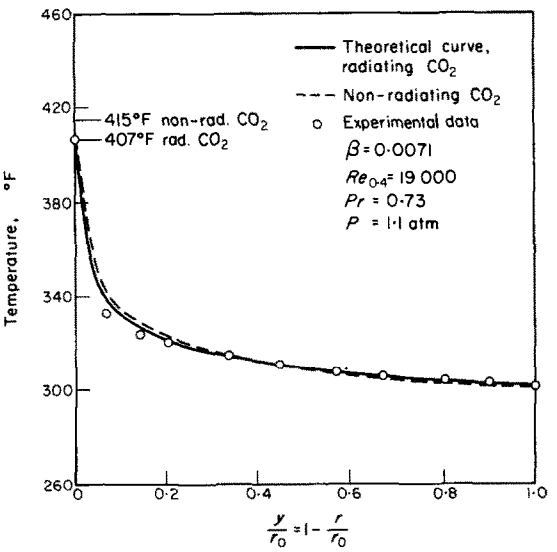

FIG. 9. Experimental and theoretical temperature profiles for carbon dioxide.

was solved numerically for the temperature profile by successive substitution.*

DISCUSSION OF EXPERIMENTAL AND THEORETICAL RESULTS

To provide a check on our experimental system and some of our fundamental theoretical assumptions, air was first used for the flowing gas. At the temperatures attained (less than 750°F) air is transparent. Temperature profiles were measured at a location 108 tube diameters downstream. A comparison between the experimental and theoretical temperature profiles is made in Figs. 4 and 5, and the agreement is seen to be very good. In particular, note the excellent agreement for the wall temperature. The runs

Table 2. Summary of results

Gas	Pressure (atm)	$Re_{0.4}$	β	$Nu_{0.4}$* (expt., non-rad.)	$Nu_{0.4}$* (theor., non-rad.)	Run no.
Air	1·1	12 200	0·0091	37·1	36·5	8
Air	1·1	14 700	0·0066	42·7	42·0	9
Gas	Pressure (atm)	$Re_{0.4}$*	β	$Nu_{0.4}$* (exp., rad.)	$Nu_{0.4}$* (theor., non-rad.)	Run no.
CO_2	1·1	12 200	0·0092	39·8	36·7	36
CO_2	1·1	16 200	0·0092	48·5	45·9	24
CO_2	1·1	19 000	0·0071	52·8	48·2	22

* Based on $T_{0.4} = T_b + 0.4(T_w - T_b)$.

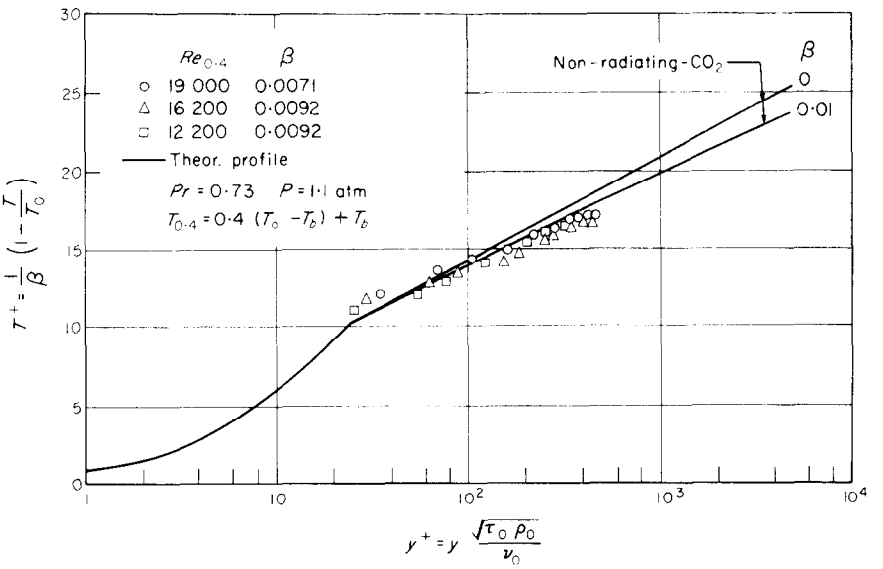

FIG. 10. Dimensionless temperature profiles for carbon dioxide.

* The details are presented in [10].

are also presented in Fig. 6 on a non-dimensional basis and the corresponding Nusselt numbers are given in Table 2.

The experimental and theoretical results for carbon dioxide are presented in Figs. 7–9 and the agreement is seen to be very good. Note, in particular, the excellent agreement for the wall temperature. It is also of interest to compare the results with a hypothetical non-radiating curve for carbon dioxide; that is, when the energy is transferred solely by conduction and convection. These curves are presented in Figs. 7–9. For a given case, both the radiating and the non-radiating curves correspond to the same heat flux, q_0, and mass flow rate, $\dot{m}$, so that the bulk temperature is the same. Now, when radiation effects are present both the temperature at the wall and the magnitude of the temperature gradient at the wall $|(dT/dy)_0|$ should be less. Furthermore, in some region away from the surface, the temperature of the radiating gas should be greater than the temperature of the transparent gas in order to obtain the same bulk temperature. Thus, the radiating and non-radiating temperature profiles should intersect. The above mentioned effects may be observed in Figs. 7–9. The experimental results are also presented in Fig. 10 on a non-dimensional basis along with the theoretical non-radiating results.

From the preceding discussion we note that the Nusselt number, defined by $q_0D/k(T_0 - T_b)$, should be greater for the flowing radiating gas than for the non-radiating case. This is consistent with our results which are summarized in Table 2.

ACKNOWLEDGEMENT

Support for this study from the National Science Foundation is gratefully acknowledged.

REFERENCES

1. R. VISKANTA, Radiation transfer and interaction of convection with radiation heat transfer, *Advances in Heat Transfer*, edited by T. F. IRVINE, JR. and J. P. HARTNETT, Vol. III, p 175. Academic Press, New York (1966).
2. C. S. LANDRAM, R. GREIF and I. S. HABIB, Heat transfer in turbulent pipe flow with optically thin radiation, *J. Heat Transfer* **91**, 330–336 (1969).
3. I. S. HABIB and R. GREIF, Non-gray radiative transport in a cylindrical medium, *J. Heat Transfer* **92**, 28–32 (1970).
4. R. D. CESS, P. MIGHDOLL and S. N. TIWARI, Infrared radiative heat transfer in non-gray gases, *Int. J. Heat Mass Transfer* **10**, 1521–1532 (1967).
5. K. H. WILSON and R. GREIF, Radiation transport in atomic plasmas, *J. Quant. Spectros. Radiat. Transfer* **8**, 1061–1086 (1968).
6. R. GREIF and I. S. HABIB, Infrared radiation transport: exact and approximate results, *J. Heat Transfer* **91**, 282–284 (1969).
7. D. K. EDWARDS and W. A. MENARD, Comparison of models for correlation of total band absorption, *Appl. Optics* **3**, 621–625 (1964).
8. C. L. TIEN and J. E. LOWDER, A correlation for total band absorptance of radiating gases, *Int. J. Heat Mass Transfer* **9**, 698–701 (1969).
9. C. L. TIEN, Thermal radiation properties of gases, *Advances in Heat Transfer*, Vol. V. Academic Press, New York (1968).
10. I. S. HABIB, Heat transfer to a radiating gas flowing turbulently in a tube: An experimental and theoretical study, Ph.D. Dissertation, University of California, Berkeley, 1968.
11. R. G. DEISSLER and C. S. EIAN, Analytic and experimental investigation of fully developed turbulent flow of air in a smooth tube with heat transfer with variable fluid properties, NACA Tech. Note 2629 (February 1952).
12. R. G. DEISSLER, Analysis of turbulent heat transfer and flow in the entrance regions of smooth passages, NACA Tech. Note 3016 (October 1953).
13. L. D. NICHOLS, Temperature profile in the entrance region of an annular passage considering the effects of turbulent convection and radiation, *Int. J. Heat Mass Transfer* **8**, 589 (1965), also see, Analytical and experimental determination of the fluid temperature profile in the entrance region of an annular passage considering the effect of convection and radiation, Case Inst. of Tech. Ph.D. Dissertation (1963).
14. R. C. MARTINELLI, Heat transfer to molten metals, *Trans. Am. Soc. Mech. Engrs* **69**, 947–959 (1947).
15. R. GREIF, Nongray radiation heat transfer in the optically thin region, *J. Heat Transfer* **90**, 363–365 (1968).
16. J. HILSENRATH, C. W. BECKETT, W. S. BENEDICT, L. FANO, H. J. HOGE, J. F. MASI, R. L. NUTTALL, Y. S. TOULOUKIAN and H. W. WOOLEY, Tables of thermal properties of gases, U.S. Dept. of Commerce, NBS Circular 564, 1955.
17. N. V. TSEDERBERG, *Thermal Conductivity of Gases and Liquids*. M.I.T. Press, Cambridge (1965).
18. C. S. LANDRAM, Combined gaseous radiative transfer and variable properties effects on Nusselt number for turbulent flow through a heated tube, Ph.D. Dissertation, Department of Mechanical Engineering, University of California, Berkeley, Calif. (1967).

ETUDE EXPÉRIMENTALE ET THÉORIQUE DU TRANSPORT DE CHALEUR VERS UN GAZ EN ÉCOULEMENT AVEC RAYONNEMENT NON-GRIS

Résumé—Le problème considéré est la détermination du transport de chaleur dans l'écoulement turbulent entièrement établi d'un gaz avec rayonnement non-gris dans un tuyau circulaire. Des résultats expérimentaux et théoriques ont été obtenus et sont en bon accord. On décrit les effets du rayonnement sur le profil de température et le nombre de Nusselt.

WÄRMEÜBERGANG AUF EIN STRÖMENDES NICHT-GRAU-STRAHLENDES GAS

Zusammenfassung—Untersucht wird der Wärmeübergang auf ein nicht-grau-strahlendes Gas in einem Rohr mit Kreisquerschnitt bei voll entwickelter turbulenter Strömung. Die experimentellen und theoretischen Ergebnisse stimmen gut überein. Es werden die Strahlungseffekte auf das Temperaturprofil und die Nusselt-Zahl angegeben.

ТЕПЛООБМЕН ПОТОКА НЕСЕРОГО ИЗЛУЧАЮЩЕГО ГАЗА

Аннотация—Исследуется теплообмен в полностью развитом турбулентном потоке несерого излучающего газа в круглой трубе. Полученные экспериментальные данные соответствуют теоретическим результатам. Приводятся данные о влиянии излучения на профиль температуры и число Нуссельта.